Mon. Not. R. Astron. Soc. **356,** 665–670 (2005) doi:10.1111/j.1365-2966.2004.08488.x

Near-infrared identification of the counterpart to X1908+075: a new OB-supergiant X-ray binary

T. Morel[1]★ and Y. Grosdidier[2,3]

[1]*Istituto Nazionale di Astrofisica, Osservatorio Astronomico di Palermo G. S. Vaiana, Piazza del Parlamento 1, I-90134 Palermo, Italy*
[2]*Instituto de Astrofísica de Canarias, Calle Vía Láctea s/n, E-38200 La Laguna (Tenerife), Spain*
[3]*Department of Physics, McGill University, 3600 University St., Montréal, Québec, Canada, H3A 2T8*

Accepted 2004 October 7. Received 2004 October 7; in original form 2004 June 18

ABSTRACT

We report the near-infrared (near-IR) identification of the likely counterpart to X1908+075, a highly absorbed Galactic X-ray source recently suspected to belong to the rare class of OB supergiant–neutron star binary systems. Our JHK_s-band imaging of the field reveals the existence within the X-ray error boxes of a near-IR source consistent with an early-type star lying at $d \sim 7$ kpc and suffering $A_V \sim 16$ mag of extinction, the latter value being in good agreement with the hydrogen column density derived from modelling of the X-ray spectrum. Our follow-up, near-IR spectroscopic observations confirm the nature of this candidate and lead to a late O-type supergiant classification, thereby supporting the identification of a new Galactic OB-supergiant X-ray binary.

Key words: stars: early-type – infrared: stars – X-rays: binaries – X-rays: individual: X1908+075.

1 INTRODUCTION

The class of high-mass X-ray binaries (HMXRBs) is defined as systems made up of a compact object (generally a neutron star) accreting material from the wind of an early-type companion, either an OB supergiant or a Be star (in which case X-ray outbursts occur when the neutron star passes through the circumstellar disc). Although the vast majority of the HMXRBs are identified as Be/X-ray binaries, the few systems with an OB supergiant primary are of particular interest. First, these objects might ultimately lead to the formation of a neutron star–black hole system and are thus important in the context of massive binary star evolution. Secondly, the disturbance induced by the orbital motion of the collapsed object through the primary stellar outflow can be used to probe the structure and physical properties of radiation-driven winds (e.g. Haberl, White & Kallman 1989; Kaper, Hammerschlag-Hensberge & van Loon 1993). To date, however, only a handful of OB-supergiant X-ray binary systems have been optically identified (Liu, van Paradijs & van den Heuvel 2000). Therefore, there is a need to uncover other members of this important population.

The Galactic X-ray source X1908+075 was first detected using the *Uhuru* satellite (Forman et al. 1978) and has been persistently catalogued ever since by several X-ray missions. These observations are summarized by Wen, Remillard & Bradt (2000, hereafter WRB) who present a variability study of this source using the All-Sky Monitor (ASM) onboard the *Rossi X-Ray Timing Explorer* (*RXTE*) satellite. The X-ray power ($\langle L_X \rangle \sim 5 \times 10^{36}$ erg s^{-1} in the 5–100 keV energy band for an adopted distance of 7 kpc and $A_V \sim 15$ mag) showed a coherent, energy-dependent sinusoidal modulation (± 30 per cent in the 5–12 keV energy band) over 3 yr with a period of 4.400 ± 0.001 d. This value is best interpreted as the orbital period of a binary system, but seems too long to be associated with a low-mass X-ray binary. The X-ray luminosity is also typical of other HMXRBs, but the smooth and regular nature of the X-ray light curve argues against a transient Be–neutron star binary system. These arguments suggest that the mass-donor star is an OB-type supergiant, while the hard X-ray spectrum supports a neutron star companion. Levine et al. (2004) recently discussed pointed observations of X1908+075 carried out with the Proportional Counter Array (PCA) and the High Energy X-ray Timing Experiment (HEXTE) onboard *RXTE*. Their analysis confirmed the modulation of the X-ray flux according to the 4.400-d orbital period, but also revealed the existence of pulsed emission with a period of 605 s. The location of X1908+075 in the pulse period/orbital period plane clearly indicates that it is a wind-fed accretion system (Corbet 1986). The mass function derived from the Doppler delay curve, along with an estimate of the orbital inclination angle derived from modelling of the orbital phase-dependence of the X-ray flux ($38^\circ \lesssim i \lesssim 72^\circ$), led to a mass of the primary in the range 9–31 $M_\odot$ and an upper limit on its size of about 22 $R_\odot$. After assumptions about the outflow dynamics, the wind column density estimates were used to derive a wind mass-loss rate, $\dot{M}$, exceeding $1.3 \times 10^{-6}\,M_\odot$ yr^{-1}. Based on the inferred stellar parameters and high mass-loss rate, they further hypothesized that the mass donor could be a Wolf–Rayet star.

The *Einstein* Imaging Proportional Counter (IPC) has localized this X-ray source at $19^h\,10^m\,46^s$ and $+07^\circ\,36'\,07''$ (J2000) with an uncertainty of about 50 arcsec. Additional constraints on the position

★E-mail: morel@astropa.unipa.it

are provided by observations made with the modulation collimator experiment (A-3) onboard the *HEAO 1* satellite (see WRB).[1] This relatively small error box offers promising prospects for seeking the counterpart, although the very high dust obscuration resulting both from the presumably large distance and from the location close to the Galactic plane ($b \sim -0.8^\circ$) prevents any follow-up studies in the optical. Here we present near-infrared (IR) imaging and spectroscopic observations identifying the likely counterpart to this X-ray source as a late O-type supergiant.

2 OBSERVATIONS AND RESULTS

2.1 Imaging

We obtained JHK_s-band images of the field on service observing mode on 2001 August 9 (JD 2452 131.50) with the IR camera CAIN-II mounted on the Carlo Sánchez Telescope (TCS) at Teide Observatory (Canary Islands, Spain). The observations were carried out under photometric sky conditions and a seeing of about 1.6 arcsec. In the adopted configuration, the plate scale is 1 arcsec pixel^{-1} and the field of view is 4.2×4.2 arcmin^2.

Standard reduction procedures for near-IR imaging were applied (multiplication by a bad pixel mask, bias subtraction, removal of pixel-to-pixel sensitivity variations in the array). A mean sky frame was created by applying a median filtering procedure to the data frames themselves. After subtraction of this mean sky frame, the individual science images (which were obtained in a dither sequence with a spatial offset of 64 arcsec) were aligned and mosaicked. The astrometric calibration was achieved with reference to the positions of 16 field stars in the USNO-A2.0 catalogue. The internal astrometric errors are of the order of 0.35 arcsec, as judged from the residuals between the measured and catalogued positions of the reference stars. The near-IR images, along with an optical image taken from the Digitized Sky Survey, are shown in Fig. 1. Our images reach a limiting magnitude in all three bands comparable to the 2MASS data, but our resolution is considerably higher owing to the poor weather conditions experienced during the 2MASS observations (seeing $\sim$2.6 arcsec).

The stellar magnitudes were computed for the stars detected at the 3σ level using the task PHOT in the IRAF[2] photometric package APPHOT. The stellar magnitudes were determined by integrating the counts through a circular aperture with a fixed radius of 3 pixel. This value provides a robust estimate of the stellar flux, while minimizing the contribution of background noise. The local sky level was estimated in a nearby, concentric annular region. The faint standard star FS35 was used for calibration (Hunt et al. 1998).[3] A subsequent correction for atmospheric extinction was applied. The limiting magnitudes for a 3σ detection in the science frames are about 17.8, 16.5 and 16.5 mag in J, H and K_s, respectively. The counterpart is expected to be detected in all three bands if we consider an early-type star with the distance and amount of interstellar absorption inferred from the X-ray data.

The colour–colour and colour–magnitude diagrams for the stars in common between the *Einstein* and *HEAO 1* error boxes are shown in Fig. 2 (we also plot, using different symbols, the three brightest sources to the south-east of the field lying within the *HEAO 1* error box, but just outside the *Einstein* error circle). To isolate the potential counterparts, we have indicated the expected positions of two representative early-type stars (O5 V and O9 I) lying at $d = 7 \pm 3$ kpc and suffering $A_V = 15 \pm 5$ mag of extinction (WRB). These rather generous uncertainties are somewhat arbitrary and are only intended to lead to a conservative pre-selection of the counterparts. Three candidates (hereafter A, B and C; see also Fig. 1 for their positions) appear to have near-IR properties consistent with the assumed distance and amount of visual extinction. Candidate C, however, formally lies outside the intersection of the two X-ray error boxes. The coordinates and near-IR magnitudes of these three potential counterparts are quoted in Table 1.

2.2 Spectroscopy

Follow-up, medium-resolution HK-band spectroscopy of the two prime candidates A and B was obtained on service observing mode on 2002 May 24 with the near-IR spectrograph CGS4 mounted on the United Kingdom Infrared Telescope (UKIRT). The sky was photometric and the seeing in the range 0.4–0.6 arcsec. The observations were carried out at JD 2 452 419.04, which corresponds to an orbital phase $\phi \sim 0.07$ according to the ephemeris of Levine et al. (2004) for a circular orbit: $\mathcal{P} = 4.4006 \pm 0.0006\,d$ and $T_{90} = 2452\,643.8$ (zero phase is fixed at minimum X-ray flux, i.e. at superior conjunction of the neutron star). We used the 300-mm focal length camera, a 0.6-arcsec wide slit and the 40 lines mm^{-1} grating in the first order (resolving power $R \sim 800$ at 2 μm). The spectral range covered in a single exposure is 1.60–2.24 μm. The slit of the spectrograph was oriented east–west, except for candidate B (PA $= -15^\circ$, i.e. nearly north–south) in order to avoid contamination from a faint near-IR source immediately lying to the east (see Fig. 1). Several background-limited exposures (for a total integration time amounting to 150 and 300 s for candidates A and B, respectively) were obtained while nodding along the slit.

Initial reduction tasks (application of the bad pixel mask, dark and bias subtraction, as well as flat-fielding) were carried out with the CGS4 data reduction pipeline ORAC-DR. Further reduction steps were carried out with the IRAF software. The OH sky lines in the science frames were removed by subtracting two-dimensional spectra obtained at different slit positions. The spectra were optimally extracted taking into account the data values and detector characteristics. An argon lamp taken at the beginning of the observations was used for the wavelength calibration. The spectra were subsequently continuum-normalized by fitting a low-order cubic spline polynomial to (pseudo) line-free regions. The removal of the telluric lines was performed using spectra of the A3 star HD 179939 obtained close in time (less than 50 min) and airmass (less than 0.03) to the target observations. The spectrum of the A star can be considered, to first order, featureless, except for the presence of the hydrogen lines of the Brackett series (Br 10–12 and Brγ in the H and K band, respectively). The procedure for removing the atmospheric telluric lines in the science spectra consisted of:

(i) interactively fitting the hydrogen lines in the telluric standard using Gaussian or Voigt profiles, paying special attention not to include the weak telluric features on both sides of the Brackett lines;

[1] Note that the position of the grid of *HEAO 1* A-3 'diamonds' in fig. 1 of WRB is incorrect (L. W. Wen, private communication). See Fig. 1 for the correct position.

[2] IRAF is distributed by the National Optical Astronomy Observatories, operated by the Association of Universities for Research in Astronomy, Inc., under cooperative agreement with the National Science Foundation.

[3] We transformed the K magnitude quoted by Hunt et al. (1998) into a K_s magnitude using equation (8) of Carpenter (2001). Although this implicitly assumes that the CAIN and 2MASS K_s-band total responses are similar, the errors arising from such an approximation are very small for a star with the colour properties of FS35 (see, e.g. equations 16 and 26 of Carpenter 2001).

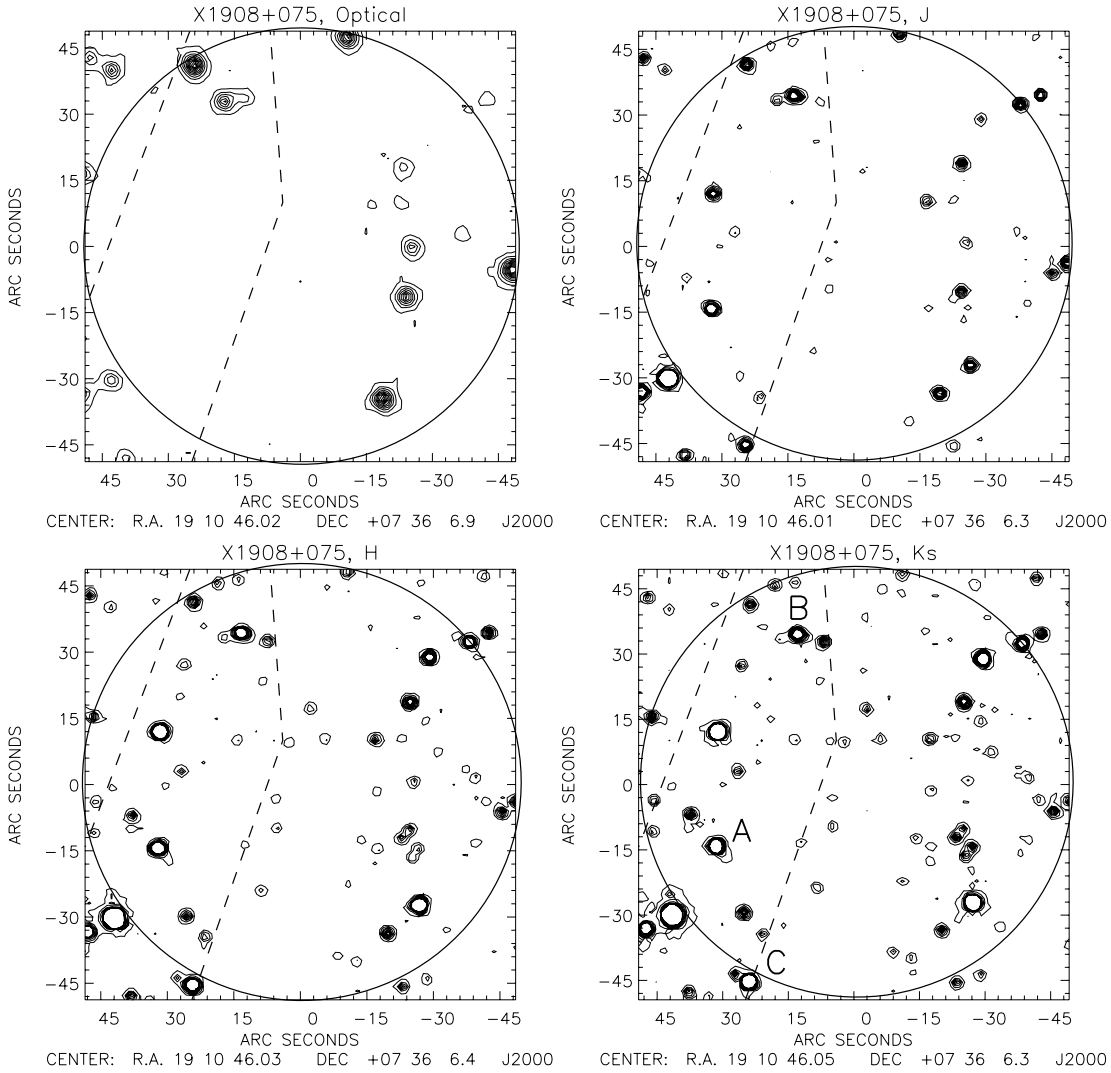

Figure 1. Contour maps of the field in the optical (image taken from a POSS-II red plate), J, H and K_s bands (the lowest contour is drawn at 3σ above the background noise, and then by steps of 6σ). The 50-arcsec error circle of the *Einstein* satellite (solid line), as well as the diamond-like error box of the *HEAO 1* satellite (dashed line) are overlayed. The IDs of the potential candidates (A, B and C, see text) are indicated in the lower, right-hand panel. North is up and east is to the left.

(ii) subtracting the fitted profiles from the A-star spectrum; and

(iii) dividing out the target spectra by this template telluric spectrum.

The typical signal-to-noise ratio estimated from the photon statistics is 130 and 60 at Brγ for candidates A and B, respectively. These figures are likely upper limits, however, considering the significant source of error arising from the unavoidably imperfect telluric correction. The *HK*-band spectra of the two candidates are shown in Fig. 3.

Although some of the weak spectral features identified in candidate B might be spurious in view of the rather limited data quality, this star clearly exhibits a large number of metallic lines absent either in candidate A or in the spectrum of a G5 star (HD 179220) taken during the same observing run (not shown). The identification of the spectral lines was mainly based on the atlases of Meyer et al. (1998) and Wallace & Hinkle (1996, 1997). The presence of the luminosity-sensitive, second-overtone ^{12}CO(6,3) band head at 1.619 μm can be taken as evidence for a cool star ($T_{\rm eff} \lesssim 5000$ K), most likely of luminosity class I–III (Meyer et al. 1998; Ivanov et al. 2004). The marginal detection of candidate B in the optical waveband suggests that it is a foreground source (Fig. 1).

The spectral morphology of candidate A is drastically different, with only evidence for hydrogen, helium and nitrogen lines. Several pieces of evidence unambiguously point to an early-type star (Hanson & Conti 1994; Hanson, Conti & Rieke 1996; Hanson, Rieke & Luhman 1998; Lenorzer et al. 2004; Hanson et al., in preparation):

(i) the emission-like N III λ2.1155 μm line is only seen in O stars and, in particular, in members of the 'Of' class, defined as showing the optical N III λλ4634, 4640 doublet in emission (Conti & Alschuler 1971);

(ii) Brγ is only in emission in O supergiant stars, *not* in O dwarfs/giants or B-type stars; and

(iii) the absence of the He II lines at 1.693 and 2.189 μm, as well as the C IV lines at 2.069, 2.078 and 2.083 μm, rules out an early O-type star; this assertion is supported by the detection of He I λ2.113 μm.

The measured strength of several diagnostic lines (see Table 2) all converge to a classification as a late O-type star, while Brγ in

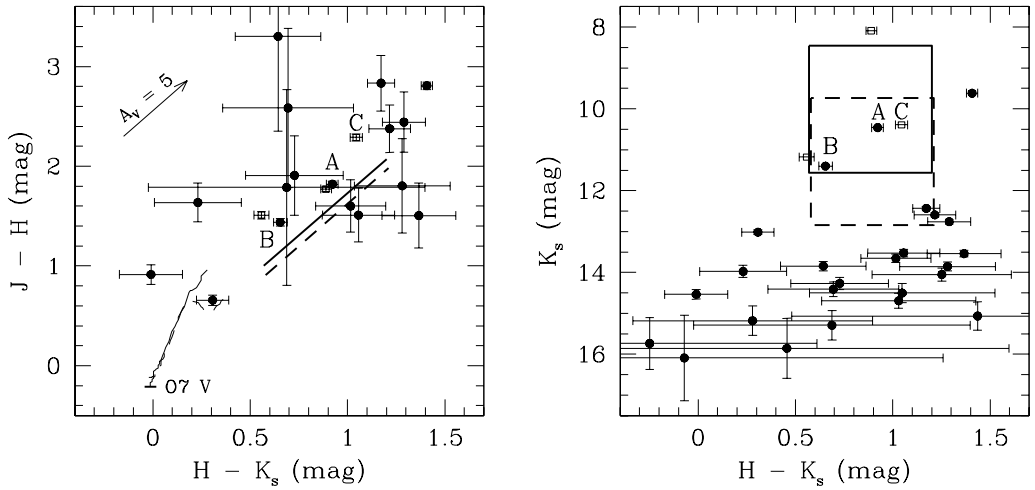

Figure 2. Colour–colour and colour–magnitude diagrams for the stars in common between the *Einstein* and *HEAO 1* error boxes (filled circles). Only stars detected in the three bands are shown. The three brightest sources to the south-east of the field lying within the *HEAO 1* error box, but just outside the *Einstein* error circle, are also plotted (open circles). The position of candidates A, B and C is indicated. The diagonal lines in the left-hand panel and the boxes in the right-hand panel show the expected loci of the near-IR counterpart to X1908+075, assuming an O5 V (dashed line) or an O9 I (solid line) star (see text). We used the calibrated M_V values and near-IR colours of Vacca et al. (1996) and Koornneef (1983), respectively. The intrinsic colours of dwarfs (dashed line) and supergiants (solid line) in the 2MASS photometric system are shown in the left-hand panel (we used the data of Koornneef 1983 and the transformation equations of Carpenter 2001). An arrow indicates the effect of reddening (near-IR interstellar extinction law from Rieke & Lebofsky 1985).

Table 1. Coordinates and near-IR magnitudes of the three potential counterparts.

ID	α (J2000)[a]	δ (J2000)[a]	J (mag)[b]	H (mag)[b]	K_s (mag)[b]
A	$19^h10^m48\overset{s}{.}204$ (21)	$+07°35'52\overset{''}{.}32$ (26)	13.199 ± 0.018	11.380 ± 0.012	10.457 ± 0.018
B	$19^h10^m46\overset{s}{.}923$ (18)	$+07°36'41\overset{''}{.}13$ (30)	13.492 ± 0.021	12.054 ± 0.014	11.399 ± 0.021
C	$19^h10^m47\overset{s}{.}713$ (28)	$+07°35'20\overset{''}{.}91$ (26)	13.721 ± 0.025	11.432 ± 0.012	10.387 ± 0.018

Notes. [a]The numbers given in parentheses are the 1σ uncertainties in the last decimal places. They take into account the typical astrometric uncertainty of the USNO-A2.0 catalogue ($\sim$0.25 arcsec), as well as differences in the relative position of the source in the J, H and K_s frames. The coordinates of candidate A differ by $\sim$0.7 arcsec from the values quoted in the 2MASS Point Source Catalogue.
[b]Note that these values may be slightly affected by nearby, faint near-IR sources (see Fig. 1). The quoted errors are the 1σ uncertainties.

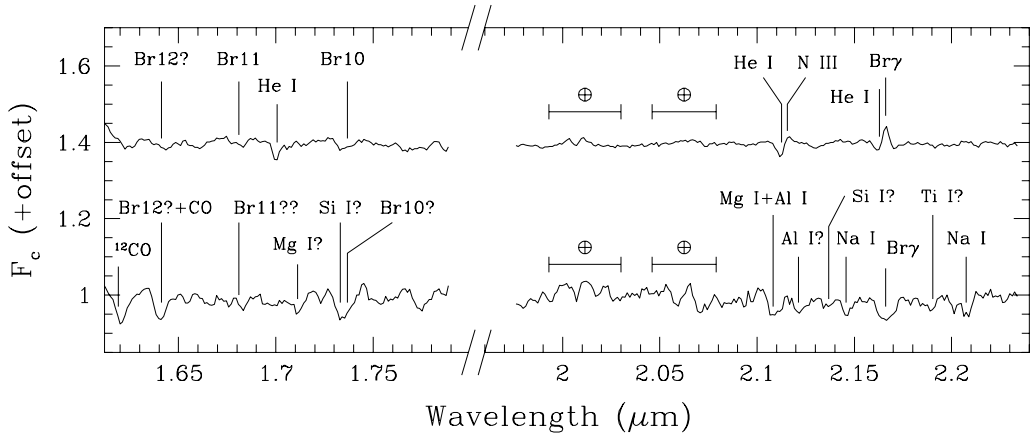

Figure 3. Continuum-normalized *HK*-band spectra of candidates A (top) and B (bottom). The spectrum of candidate A has been shifted along the ordinate axis by 0.4 continuum units. The most prominent spectral features are labelled (uncertain identifications are indicated by a question mark). The line wavelengths and EWs of the lines identified in candidate A are quoted in Table 2. The reader is referred to Lançon & Rocca-Volmerange (1992), Meyer et al. (1998) and Wallace & Hinkle (1996, 1997) for further details regarding the features identified in candidate B. The $\oplus$ symbols mark the position of the strong CO_2 telluric lines. Some spurious features arising from an imperfect telluric subtraction can be seen at these locations.

emission diagnoses a supergiant (Hanson et al. 1996, 1998). Based on these arguments, we propose a O7.5–O9.5 If classification. The *K*-band spectral morphology is reminiscent of HD 57060 (O7 Iafp) or HD 151804 (O8 Iaf; Hanson et al. 1996). Similarities are also found with HD 123008 (ON9.5 Iab), for instance (Hanson et al., in preparation). The most conspicuous difference is the absence in X1908+075 of the He I λ2.058 μm line, as observed in other OB-supergiant X-ray binaries (e.g. Cyg X-1; Hanson et al. 1996).

Table 2. Line properties of X1908+075.

Line	EW (Å)
Br 12 λ1.6412	+1.4
Br 11 λ1.6810	+0.8
He I λ1.7007	+1.9
Br 10 λ1.7367	+1.5
He I λ2.1127	+1.2
N III λ2.1155	−0.6
He I λ2.163	+0.7
Brγ λ2.1661	−1.4

Setting stringent limits on the strength on this feature is hampered by the existence of a strong telluric band stretching from 2.045 to 2.080 μm. If present, however, the helium line is clearly very weak. We note the lack of a clear relationship in O stars between the strength of this feature and the spectral type (Hanson et al. 1996). This peculiar behaviour may result from the sensitivity of this line to the extreme UV flux, for instance (e.g. Najarro et al. 1994).

The question naturally arising is to what extent a classification scheme based on 'normal' OB stars can be confidently used for stars harbouring a compact object. Despite the fact that Hanson et al. (1996) obtained *K*-band spectra of several HMXRBs and did not find clear evidence for spectral peculiarities compared to single stars with the same optical classification, we cannot certainly rule out that the presence of the neutron star affects in some way our spectral classification. However, the fact that all diagnostic lines yield consistent results gives us confidence in our results. Furthermore, a circular orbit would imply that our spectroscopic observations were secured close to superior conjunction of the neutron star (see Section 2.2). Were it to be the case, this fortunate circumstance would imply that the spectral type we derive is not strongly biased by the X-ray irradiated part of the photosphere of the primary.

3 DISCUSSION

Although phase-locked photometric variations might be expected in X1908+075, our near-IR magnitudes appear to be compatible with the 2MASS Point Source Catalogue data (observations obtained at JD 2451 394.61; designation 2MASS 19104821+0735516): $J = 13.228 \pm 0.021$, $H = 11.457 \pm 0.027$ and $K_s = 10.480 \pm 0.022$ mag. Using the absolute magnitudes appropriate for an O9 I star (Koornneef 1983; Vacca, Garmany & Shull 1996) and the near-IR interstellar extinction law of Rieke & Lebofsky (1985), we obtain from our data: $d \sim 7$ kpc and $A_V \sim 16.5$ mag. WRB and Levine et al. (2004) derived a column density of intervening interstellar material to the source in the range $N_{\rm H} = 3.0$–4.6×10^{22} atoms cm^{-2} from a modelling of the X-ray spectrum. This translates into an amount of interstellar extinction, $A_V = 16.0$–24.6 mag (Bohlin, Savage & Drake 1978). This range of values is in reasonable agreement with our estimate considering the large uncertainties involved, for instance, in the empirical transformation between the hydrogen column density and the optical extinction in the *V* band. X1908+075 is undetected on a POSS-II red plate going down to $R \sim 20$ mag (see Fig. 1), in accordance with our derived spectral type, distance and amount of interstellar extinction (we expect $R \sim 24.5$ mag for $A_V \sim 16.5$ mag, $M_V = -6.5$ and $V - R = -0.15$; Vacca et al. 1996).

Levine et al. (2004) estimated the following physical parameters for the primary star based on *RXTE* data: $M_\star = 9$–$31\,{\rm M}_\odot$, $R_\star \lesssim 22\,{\rm R}_\odot$ and $\dot{M} \gtrsim 1.3 \times 10^{-6}\,{\rm M}_\odot\,{\rm yr}^{-1}$. The constraint on the stellar radius, together with the high mass-loss rate inferred, led them to propose that the massive component could be a Wolf–Rayet star. This interpretation is, however, not supported by the lack in X1908+075 of strong, broad emission lines (see, e.g. Morris et al. 1996; Figer, McLean & Najarro 1997). Because Wolf–Rayet stars have absolute magnitudes and colours comparable to O-type supergiants, it is likely that such an object would have been isolated by its photometric properties (Fig. 2). Although perhaps not compelling in itself, systems made up of a Wolf–Rayet star and a compact companion are expected to have short orbital periods following a spiral-in phase (e.g. de Donder, Vanbeveren & van Bever 1997). A period of 4.8 hr is observed in Cygnus X-3, the prime candidate for such a system (van Kerkwijk et al. 1996).

The most stringent constraint coming from the X-ray data is the fact that the neutron star is accreting material well below the Eddington rate. This implies that the companion is wind-fed and lies within the Roche lobe, i.e. $R_\star \lesssim 22\,{\rm R}_\odot$. Optical radial velocity curves have been combined with X-ray eclipse data by van Kerkwijk, van Paradijs & Zuiderwijk (1995) to derive accurate masses and radii for three B0–B0.5 supergiants in X-ray binaries. They derived $R_\star \sim 30\,{\rm R}_\odot$ and $M_\star \sim 24\ {\rm M}_\odot$ for Vela X-1, while $R_\star \sim 15\ {\rm R}_\odot$ and $M_\star \sim 15\,{\rm M}_\odot$ was found for 4U 1538–52 and SMC X-1. This shows that a supergiant classification does not enter in conflict with the upper limit on the stellar radius, although it is likely that X1908+075 is close to filling its Roche lobe, as commonly observed in these systems.

Mass-loss rates of late O-type supergiants measured from the radio free–free emission or from the strength of the Hα line typically lie in the range 1–$10 \times 10^{-6}\,{\rm M}_\odot\ {\rm yr}^{-1}$ (e.g. Leitherer 1988; Lamers & Leitherer 1993). Theoretical models of radiation-driven winds predict an *inverse* dependence of the mass-loss rate with the stellar mass (e.g. Abbott 1982). The value $\dot{M} \gtrsim 1.3 \times 10^{-6}\,{\rm M}_\odot\ {\rm yr}^{-1}$ derived by Levine et al. (2004) is thus entirely conceivable considering that X1908+075 has a lower mass than the stars discussed above. However, a comparable luminosity is required for this object: typically $\log(L_\star/{\rm L}_\odot) \gtrsim 5.2$ (Vink, de Koter & Lamers 2000). We note that the N III λ2.116 line in emission suggests an evolved O star with a very high luminosity and a rather strong stellar wind (Conti & Alschuler 1971).

4 CONCLUSION

The use of several diagnostic lines in the *HK* windows has led to a robust classification of the likely counterpart to X1908+075 as a late O-type star, while Brγ in emission strongly points to a supergiant (Hanson et al. 1996). The proposed O7.5–O9.5 If spectroscopic classification is internally consistent with the near-IR photometric properties and also compatible with the stellar parameters independently derived by Levine et al. (2004) from X-ray data, provided that the star satisfies $\log(L_\star/{\rm L}_\odot) \gtrsim 5.2$. As mentioned previously, the X-ray data do not argue in favour of a Be/X-ray binary system. The lack of strong near-IR emission lines in X1908+075 strongly supports this conclusion (Everall et al. 1993). Despite the prohibitively high visual extinction, further advances in our understanding of this system may come from radio or time-resolved near-IR observations, the latter both in the photometric and spectroscopic modes. Further X-ray observations with higher spatial resolution, as well as near-IR spectroscopic data for other possible candidates in the field (notably candidate C; see Figs 1 and 2), are also needed for an unambiguous identification of the counterpart. In this regard, we point out that the lack of evidence for an embedded young cluster in the line of sight

to X1908+075 (Bica et al. 2003, and references therein) strengthens the case for a correct identification.

ACKNOWLEDGMENTS

We thank A. M. Levine for constructive and fruitful discussions during the course of this work. We also wish to thank the anonymous referee and D. F. Figer for useful comments, as well as M. M. Hanson for making her manuscript available to us prior to publication. The imaging data used in this paper were obtained as part of the Teide Observatory Service Observing Programme. The United Kingdom Infrared Telescope is operated by the Joint Astronomy Centre on behalf of the UK Particle Physics and Astronomy Research Council. The spectroscopic data reported here were obtained as part of the UKIRT Service Programme. The Digitized Sky Survey was produced at the Space Telescope Science Institute (STScI) under US government grant NAGW-2166. The images of these surveys are based on photographic data obtained using the Oschin–Schmidt Telescope on Palomar Mountain and the UK Schmidt Telescope. The plates were processed into the present compressed digital form with the permission of these institutions. This publication makes use of data products from the Two Micron All Sky Survey, which is a joint project of the University of Massachusetts and the Infrared Processing and Analysis Center/California Institute of Technology, funded by the National Aeronautics and Space Administration and the National Science Foundation.

REFERENCES

Abbott D. C., 1982, ApJ, 259, 282
Bica E., Dutra C. M., Soares J., Barbuy B., 2003, A&A, 404, 223
Bohlin R. C., Savage B. D., Drake J. F., 1978, ApJ, 224, 132
Carpenter J. M., 2001, AJ, 121, 2851
Conti P. S., Alschuler W. R., 1971, ApJ, 170, 325
Corbet R. H. D., 1986, MNRAS, 220, 1047
de Donder E., Vanbeveren D., van Bever J., 1997, A&A, 318, 812
Everall C., Coe M. J., Norton A. J., Roche P., Unger S. J., 1993, MNRAS, 262, 57
Figer D. F., McLean I. S., Najarro F., 1997, ApJ, 486, 420
Forman W., Jones C., Cominsky L., Julien P., Murray S., Peters G., Tananbaum H., Giacconi R., 1978, ApJS, 38, 357
Haberl F., White N. E., Kallman T. R., 1989, ApJ, 343, 409
Hanson M. M., Conti P. S., 1994, ApJ, 423, L139
Hanson M. M., Conti P. S., Rieke M. J., 1996, ApJS, 107, 281
Hanson M. M., Rieke G. H., Luhman K. L., 1998, AJ, 116, 1915
Hunt L. K., Mannucci F., Testi L., Migliorini S., Stanga R. M., Baffa C., Lisi F., Vanzi L., 1998, AJ, 115, 2594
Ivanov V. D., Rieke M. J., Engelbracht C. W., Alonso-Herrero A., Rieke G. H., Luhman K. L., 2004, ApJS, 151, 387
Kaper L., Hammerschlag-Hensberge G., van Loon J. Th., 1993, A&A, 279, 485
Koornneef J., 1983, A&A, 128, 84
Lamers H. J. G. L. M., Leitherer C., 1993, ApJ, 412, 771
Lançon A., Rocca-Volmerange B., 1992, A&AS, 96, 593
Leitherer C., 1988, ApJ, 326, 356
Lenorzer A., Mokiem M. R., de Koter A., Puls J., 2004, A&A, 422, 275
Levine A. M., Rappaport S., Remillard R., Savcheva A., 2004, ApJ, in press (astro-ph/0404428)
Liu Q. Z., van Paradijs J., van den Heuvel E. P. J., 2000, A&AS, 147, 25
Meyer M. R., Edwards S., Hinkle K. H., Strom S. E., 1998, ApJ, 508, 397
Morris P. W., Eenens P. R. J., Hanson M. M., Conti P. S., Blum R. D., 1996, ApJ, 470, 597
Najarro F., Hillier D. J., Kudritzki R. P., Krabbe A., Genzel R., Lutz D., Drapatz S., Geballe T. R., 1994, A&A, 285, 573
Rieke G. H., Lebofsky M. J., 1985, ApJ, 288, 618
Vacca W. D., Garmany C. D., Shull J. M., 1996, ApJ, 460, 914
van Kerkwijk M. H., van Paradijs J., Zuiderwijk E. J., 1995, A&A, 303, 497
van Kerkwijk M. H., Geballe T. R., King D. L., van der Klis M., van Paradijs J., 1996, A&A, 314, 521
Vink J. S., de Koter A., Lamers H. J. G. L. M., 2000, A&A, 362, 295
Wallace L., Hinkle K. H., 1996, ApJS, 107, 312
Wallace L., Hinkle K. H., 1997, ApJS, 111, 445
Wen L., Remillard R. A., Bradt H. V., 2000, ApJ, 532, 1119 (WRB)

This paper has been typeset from a TEX/LATEX file prepared by the author.